Effects of hole scattering on two-photon photoemission from metal surfaces

Mamoru Sakaue* and Toshiaki Munakata
RIKEN (The Institute of Physical and Chemical Research), Wako, Saitama 351-0198, Japan

Hideaki Kasai and Ayao Okiji
Graduate School of Engineering, Osaka University, Suita, Osaka 565-0871, Japan
(Received 4 June 2003; published 21 November 2003)

By the nonequilibrium Green function method, we investigate the effects of the inelastic scattering of photoexcited holes at metal surfaces on the two-photon photoemission (2PPE) spectra. The 2PPE spectra of a metal surface we study show two peaks attributed to an occupied localized state (2ω peak) and an unoccupied localized state (1ω peak). Energy transfer between the surface and the bulk due to the hole scattering accounts for the occurrence of the 1ω peak, while it is usually considered that this peak occurs due to dephasing in macroscopic theories. As well as the 1ω peak, the peak height and width of the 2ω peak, which is usually considered to occur due to a direct two-photon excitation process, are affected by the hole scattering. By comparing with a macroscopic theory based on the density matrix method, we discuss the relation of the macroscopic energy relaxation time and the dephasing time with intrinsic lifetimes of the electrons and holes in detail.

DOI: 10.1103/PhysRevB.68.205421 PACS number(s): 79.60.−i, 78.68.+m, 71.10.−w

I. INTRODUCTION

Two-photon photoemission (2PPE) spectroscopy is one of the successful experimental methods of investigating electronic structures of metal surfaces. The experimental results, i.e., 2PPE spectra, can provide information on photoinduced electron dynamics at the surfaces both in the energy and time domains. When the photon energy is close to the resonance between occupied and unoccupied states at the surface, e.g., Shockley states, image states, or atomic/molecular orbitals of adsorbates, it is known that the 2PPE spectra can exhibit peaks at $E_0+2\hbar\omega$ (2ω peak) and $E_1+\hbar\omega$ (1ω peak),[1–5] where E_0 and E_1 are the energy levels of the occupied and unoccupied states, respectively, and $\hbar\omega$ is the photon energy. It is usually considered that the 2ω peak is due to direct two-photon excitation from the occupied state to a free-electron state above the vacuum level via a virtual intermediate state, and the 1ω peak is due to one-photon excitation from the unoccupied state populated by scattering of other photoexcited electrons.[1,2,6–8]

In the usual experiments,[2,6] density matrix methods based on the Liouville–von Neumann equations (or optical Bloch equations), typically within the three-level model or its modified ones, are used for analysis of the 2PPE spectra by introducing macroscopic relaxation and dephasing times. It is usually considered that the relaxation is due to inelastic scattering and the dephasing is due to (quasi-) elastic scattering. It is known that the dephasing is necessary for the occurrence of the 1ω peak.[2,6,8] It will be explained from a macroscopic point of view that the elastic scattering causes transition from photoinduced virtual polarizations to other real polarizations at the surface.

In order to understand the microscopic mechanisms of the relaxation and dephasing at the surfaces, it is necessary to investigate the electron dynamics by methods based on the many-body theories, e.g., the nonequilibrium Green function method.[9,10] We have investigated the effects of Coulomb interactions between electrons on the temporal evolution of the electron densities[11] and the time-resolved 2PPE spectra[7] measured by applying the pump-probe technique. However, the relation between the macroscopic and the microscopic theories on the 2PPE from metal surfaces is not understood thoroughly.

In a recent work on the pump-probe cross-correlation traces (photoelectron intensities as functions of the pump-probe delay time) in the time-resolved 2PPE spectra,[12] we demonstrated in the time domain that inelastic scattering of the hole in the occupied state is concerned with the dephasing. In this paper, we investigate the relation of the hole scattering with the dephasing in the energy domain. We calculate the spectra by the nonequilibrium Green function method based on the Liouville equations where Coulomb interactions between electrons in the bulk and surface are taken into account. Absorption of the first photon of which the energy is detuned from the resonance between the occupied and unoccupied states causes a virtual electron excitation from the occupied state to the unoccupied state. Subsequently, inelastic scattering of the hole in the occupied state causes an energy transfer between the bulk and the surface, so that the state of the electron system can change to a real state in which an electron is in the unoccupied state and secondary electrons and holes are in the bulk. Then the second photon excites the electron to a free-electron state and hence the 1ω peak is formed. Based on the numerical results of the 2PPE spectra, we discuss how the photon energy dependence of the heights and widths of the peaks is related to the intrinsic lifetimes of the occupied and the unoccupied states.

II. THEORY

We introduce a system of which the Hamiltonian is described as H_0+V, where the unperturbed Hamiltonian is given by

$$H_0=\sum_{\mu} E_{\mu}c_{\mu}^{\dagger}c_{\mu}, \tag{1}$$

and the Coulomb interactions between electrons are given by

$$V=\frac{1}{2}\sum_{\kappa,\lambda,\mu,\nu} V_{\kappa\lambda/\mu\nu}c_\lambda^\dagger c_\kappa^\dagger c_\mu c_\nu . \tag{2}$$

Here κ, λ, μ, and ν are indices denoting electronic states $|\mu\rangle$ in all of the bulk, surface, and vacuum (the spin index is omitted for simplicity), and E, $c^\dagger$, and c stand for the energy, creation operator and annihilation operator, respectively. We assume that the first photon excites an electron in an occupied state $|0\rangle$ at the surface to an unoccupied state $|1\rangle$ at the surface and subsequently the second photon excites the electron to a free-electron state $|2\rangle$ above the vacuum level due to the interactions of an electron with light:

$$W(t)=W_{21}(t)c_2^\dagger c_1+W_{10}(t)c_1^\dagger c_0+\text{H.c.} \tag{3}$$

The photoelectron intensity is investigated by solving the Liouville equation for the density matrix in the Schrödinger representation:

$$i\hbar\frac{\partial\rho(t)}{\partial t}=[H_0+V+W(t),\rho(t)]. \tag{4}$$

By expanding with respect to $V+W(t)$, the photoelectron density $\rho_{22}(t)$ can be written to be a sum of multiple integrals of many-body correlation functions.[13] Then, by using the diagrammatic technique, we obtain

$$\begin{aligned}\rho_{22}(t_{ob})=&-i\hbar\int_\infty^{-\infty}dt_1'\int_\infty^{-\infty}dt_2'\int_{-\infty}^{\infty}dt_2\int_{-\infty}^{\infty}dt_1\\&\times\theta(t_{ob}-t_2')\theta(t_2'-t_1')\theta(t_{ob}-t_2)\theta(t_2-t_1)\\&\times W_{01}(t_1')W_{12}(t_2')W_{21}(t_2)W_{10}(t_1)\\&\times G_{22}^{++}(t_{ob}-t_2)G_{11}^{++}(t_2-t_1)G_{00}^{+-}(t_{ob}-t_1,t_1'-t_{ob})\\&\times G_{11}^{--}(t_1'-t_2')G_{22}^{--}(t_2'-t_{ob}),\end{aligned} \tag{5}$$

where t_{ob} is the observation time of the photoelectron and $\theta(t)$ is a step function.

Here G^{++} and G^{--} are causal and anticausal Green functions,[9] respectively, approximately given at the absolute zero of temperature by

$$\begin{aligned}G_{\mu\mu}^{++}(t-t')=&-[G_{\mu\mu}^{--}(t'-t)]^*\\\simeq&(i\hbar)^{-1}\{\theta(E_\mu-E_F)\theta(t-t')e^{(-iE_\mu-\Gamma_\mu)(t-t')/\hbar}\\&-\theta(E_F-E_\mu)\theta(t'-t)e^{(iE_\mu-\Gamma_\mu)(t'-t)/\hbar}\},\end{aligned} \tag{6}$$

where Γ_μ is a linewidth (inverse lifetime) of a state $|\mu\rangle$ and E_F is the Fermi level. G^{+-} is an interbranch Green function that strides over the forward and backward branches (corresponding to the ket and bra vectors in the Schrödinger representation, respectively) in the Keldysh contour.[9,10] This function describes the dynamical change of the secondary particle (electrons and holes in the bulk) densities and the phase correlation between the ket and bra vectors. In the usual nonequilibrium Green function method, the t_{ob} dependence is neglected and G_{00}^{+-} is assumed to be a function of t_1-t_1'. As shown in the Appendix, this assumption leads to a formula of ρ_{22} equivalent to those obtained by the density matrix method. However this assumption is shown to be inappropriate by analyzing the formula of the function in detail,[10]

$$\begin{aligned}&G_{00}^{+-}(t_{ob}-t,t'-t_{ob})\\&=-\sum_{n=0}^{\infty}\sum_{n'=0}^{\infty}\left(\frac{1}{i\hbar}\right)^{n+n'+1}\int_\infty^{-\infty}dt_1'\ldots\int_\infty^{-\infty}dt_{n'}'\\&\times\int_{-\infty}^{\infty}dt_n\ldots\int_{-\infty}^{\infty}dt_1\theta(t_{ob}-t_{n'}')\ldots\theta(t_2'-t_1')\\&\times\theta(t_{ob}-t_n)\ldots\theta(t_2-t_1)\sum_{l=1}^{n}\sum_{l'=1}^{n'}\theta(t_{l+1}-t)\\&\times\theta(t-t_l)\theta(t_{l'+1}'-t')\theta(t'-t_{l'}')\langle v(t_1')\ldots\\&\times c_0^\dagger(t')\ldots v(t_{n'}')v(t_n)\ldots c_0(t)\ldots v(t_1)\rangle,\end{aligned} \tag{7}$$

where t_{n+1} and $t_{n'+1}'$ in the summations are replaced with t_{ob}. $c_0^\dagger(t)$, $c_0(t)$, and $v(t)$ are the interaction representations of $c_0^\dagger$, c_0, and V. The statistical average at a temperature T is defined by

$$\langle\ldots\rangle=\text{Tr}[\exp(-H_0/k_BT)\ldots]/\text{Tr}[\exp(-H_0/k_BT)], \tag{8}$$

where k_B is the Boltzmann constant.

The Green function given by Eq. (7) describes the scattering of the photoexcited hole in $|0\rangle$ by Coulomb interactions between electrons. The t_{ob} dependence of G_{00}^{+-} shows that the hole scattering which occurs before t_{ob} can affect $\rho_{22}(t_{ob})$ by changing the quantum phase of the system. This Green function satisfies the equation of motion in the same way as the usual Keldysh Green functions[9] defined by assuming sufficiently large t_{ob} at which the system is in the metastable state.[10] Since the final state of 2PPE from a metal surface is not an eigenstate because of the hole scattering, it is necessary to consider the t_{ob} dependence of the Green function.

In the following, we give $W_{\mu\nu}(t)=[W_{\nu\mu}(t)]^*=W_{\mu\nu}\exp(-i\omega t)$ within the rotating wave approximation in order to obtain the energy spectra for continuous light. G_{00}^{+-} can be rewritten as a function of two energies attributed to the time evolution in the forward and backward branches by Fourier transform,

$$\begin{aligned}&G^{+-}[E,E']\\&=\int_{-\infty}^{\infty}d\tau\int_{-\infty}^{\infty}d\tau'\exp[-i(E\tau+E'\tau')/\hbar]G^{+-}(\tau,\tau'),\end{aligned} \tag{9}$$

whereas the causal and anti-causal Green functions are transformed by

$$G^{+\pm}[E]=\int_{-\infty}^{\infty}d\tau\exp(-iE\tau/\hbar)G^{\pm\pm}(\tau). \tag{10}$$

Then the photoelectron density is obtained as

$$\rho_{22}[E_2]=\frac{1}{i\hbar(2\pi)^2}|W_{21}W_{10}|^2\int_{C_+}d\epsilon_0\int_{C_-}d\epsilon_0' \times G_{22}^{++}[-2\hbar\omega-\epsilon_0-i0_+] \times G_{11}^{++}[-\hbar\omega-\epsilon_0-i0_+]G_{00}^{+-}[\epsilon_0,\epsilon_0'] \times G_{11}^{--}[-\hbar\omega-\epsilon_0'+i0_+] \times G_{22}^{--}[-2\hbar\omega-\epsilon_0'+i0_+], \quad (11)$$

where 0_+ is an infinitesimal positive value. C_+ and C_- denote the sufficiently large integration paths in the upper (positive imaginary part) and the lower (negative) sides of the complex number plane, respectively, including a path $-\infty\rightarrow\infty$. This equation is rewritten by considering G_{00}^{+-} within the typical second order diagrams[10] as

$$\rho_{22}[E_2]=|W_{21}W_{10}|^2[(E_2-E_0-2\hbar\omega)^2+(\Gamma_2+\Gamma_0)^2]^{-1}[(E_1-E_0-\hbar\omega)^2+(\Gamma_1+\Gamma_0)^2]^{-1} \times\left\{1+\sum_{\alpha}^{\text{unocc}}\sum_{\beta}^{\text{occ}}\sum_{\gamma}^{\text{occ}}[V_{\beta\gamma/q\alpha}V_{\alpha q/\gamma\beta}-V_{\beta\gamma/q\alpha}V_{\alpha q/\beta\gamma}] \times\frac{1}{(E_2+E_\alpha-E_\beta-E_\gamma-2\hbar\omega)^2+(\Gamma_2+\Gamma_\alpha+\Gamma_\beta+\Gamma_\gamma)^2}\frac{1}{(E_1+E_\alpha-E_\beta-E_\gamma-\hbar\omega)^2+(\Gamma_1+\Gamma_\alpha+\Gamma_\beta+\Gamma_\gamma)^2} \times|(E_2-2\hbar\omega-i\Gamma_2)+(E_1-\hbar\omega-i\Gamma_1)+(-E_0-i\Gamma_0)+[E_\alpha-E_\beta-E_\gamma-i(\Gamma_\alpha+\Gamma_\beta+\Gamma_\gamma)]|^2\right\}, \quad (12)$$

where the summations are taken over the states of secondary electrons and holes in the bulk. The linewidths of the bulk states and $|0\rangle$ are given by the causal Green functions defined by Eq. (6). The first term in the brace accounts for the 2ω peak due to a process where first an electron in $|0\rangle$ is photoexcited to $|1\rangle$ virtually and subsequently photoexcited to $|2\rangle$. The second term accounts for both the 1ω and 2ω peaks due to processes where, after the virtual electron photoexcitation from $|0\rangle$ to $|1\rangle$, the hole in $|0\rangle$ is scattered inelastically by bulk electrons and subsequently the electron in $|1\rangle$ is photoexcited to $|2\rangle$.

When the scattering probability of the hole in $|0\rangle$ is negligible, i.e., Γ_0 and $V_{\beta\gamma/q\alpha}V_{\alpha q/\gamma\beta}-V_{\beta\gamma/q\alpha}V_{\alpha q/\beta\gamma}$ in Eq. (12) are small, the photoexcited hole remains in $|0\rangle$ in the final state. In this case, the second term in the brace of Eq. (12) vanishes and hence ρ_{22} exhibits only the 2ω peak [the same results can be obtained by the density matrix method as shown in Eq. (A6)]. Meanwhile, when the scattering probability is large, one electron and two holes can be excited in the bulk in the final state as a result of the scattering. In this case, the second term becomes effective and hence ρ_{22} exhibits both the 1ω and 2ω peaks because of the energy transfer between the surface and the bulk due to the scattering. From a macroscopic point of view, this scattering process accounts for the transition from a virtual polarization between the electron in $|1\rangle$ and the hole in $|0\rangle$ to real polarizations between the electron in $|1\rangle$ and the bulk charges (positive in total) consisting of the secondary electrons and holes.

III. RESULTS

For example, the 2PPE energy spectra of Cu(111) where $E_0-E_F=-0.445$ eV, $\Gamma_0=12.7$ meV (Shockley state),[14] $E_1-E_F=4.12$ eV, $\Gamma_1=14.3$ meV (image state),[15] and $\Gamma_2=0$ are shown in Fig. 1. The lifetime of a bulk electron in $|\mu\rangle$ is given to be 30 fs for $|E_\mu-E_F|=1$ eV[16] within the Fermi liquid theory.[17] Here we assume a flat density of states for the bulk electrons. For simplicity, $V_{\beta\gamma/q\alpha}V_{\alpha q/\gamma\beta}-V_{\beta\gamma/q\alpha}V_{\alpha q/\beta\gamma}$ in Eq. (12) is assumed to be a constant value which gives $\Gamma_0=12.7$ meV by calculation of the self-energy within the second order with respect to V.

The obtained results reproduce the two-peak structure in the experimental 2PPE spectra[1,2] for the finite detuning $\Delta E=\hbar\omega-(E_1-E_0)\neq 0$ except for the sharp structure on the 2ω peak (at 4.22 eV for $\Delta E=+100$ meV and at 4.02 eV for $\Delta E=-100$ meV). This structure is due to the excitation of secondary electrons and holes with infinitesimal excitation energies accompanied by the quasielastic hole transfer from the surface to the bulk, i.e., a sort of the Fermi surface effects. There will be two reasons for the disagreement with the experiments concerning the sharp structure. One is the experimental condition, i.e., the finite linewidths of the laser pulses and the finite temperature of the samples. The other is the theoretical incompleteness that will be resolved by renormalization or similar techniques. Investigation on the physical validity of the occurrence of this structure will be an important future subject.

By taking notice of the photon energy dependence of the spectra, we compare the 2PPE spectra obtained by the microscopic theory based on the Green function method and the macroscopic theory (three-level model; see the Appendix) based on the density matrix method. As mentioned in the Appendix, the most remarkable difference between the Green function method and the density matrix method is seen in the estimate of the interference effects accounting for the dephasing. When the processes accounting for the two

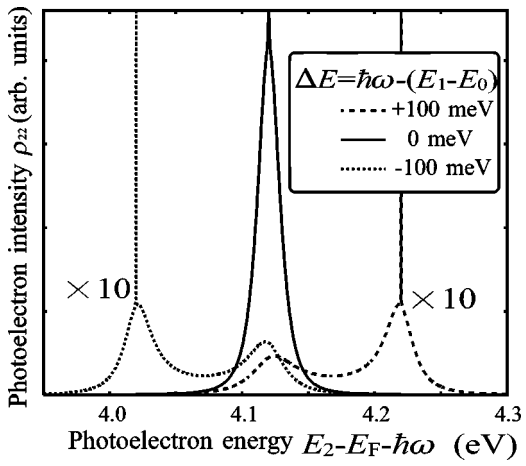

FIG. 1. 2PPE energy spectra of Cu(111) as functions of $E_2-E_F-\hbar\omega$ (so that the 1ω peak is fixed at 4.12 eV) for photon energies $\Delta E=\hbar\omega-(E_1-E_0)=-0.1$, 0, and 0.1 eV.

peaks are incoherent, the 2PPE spectra will reflect only the density of states around the occupied and the unoccupied states approximately expressed by Lorentzians. Then we fit sums of two Lorentzians to the obtained spectra in the method of least squares. Here, in the results by the Green function method, the component due to the Fermi surface effect is ignored.

The results for $\Delta E=100$ and 20 meV are shown in Fig. 2. Here, in the density matrix method, we give the inverse energy relaxation time γ_1 as Γ_1 and the inverse pure dephasing time $\bar{\gamma}$ as Γ_0. Then, as mentioned later, the 1ω and 2ω peak widths at the lowest limit of the photon energy for which the 1ω peak structure is not collapsed by the Fermi cutoff and the widths of the resonance curves (the 1ω and 2ω peak heights as functions of $\hbar\omega$) agree with those obtained by the Green function method.

When the detuning is small, the two peaks fuse together and hence the spectra exhibit one peak [see Figs. 2(a-1) and 2(b-1)]. Since the frequencies of the transition probability amplitudes of the processes accounting for the two peaks coincide with each other, the original meanings of the 1ω and 2ω peaks are lost due to the interference between the processes. However, in order to investigate the asymptotic behavior of the two peaks, we tentatively decompose the spectra into two Lorentzian components by assigning the 1ω and 2ω peak components to those at the higher and the lower energy positions for the negative detuning, respectively, and in reverse for the positive detuning. Then we see that the widths of the both components become narrower than the intrinsic linewidths ($2\Gamma_1=28.6$ eV for the 1ω and $2\Gamma_0=25.4$ eV for the 2ω) due to the interference effect.[5]

When the detuning is larger than several times the linewidths of the occupied and unoccupied states, the spectra

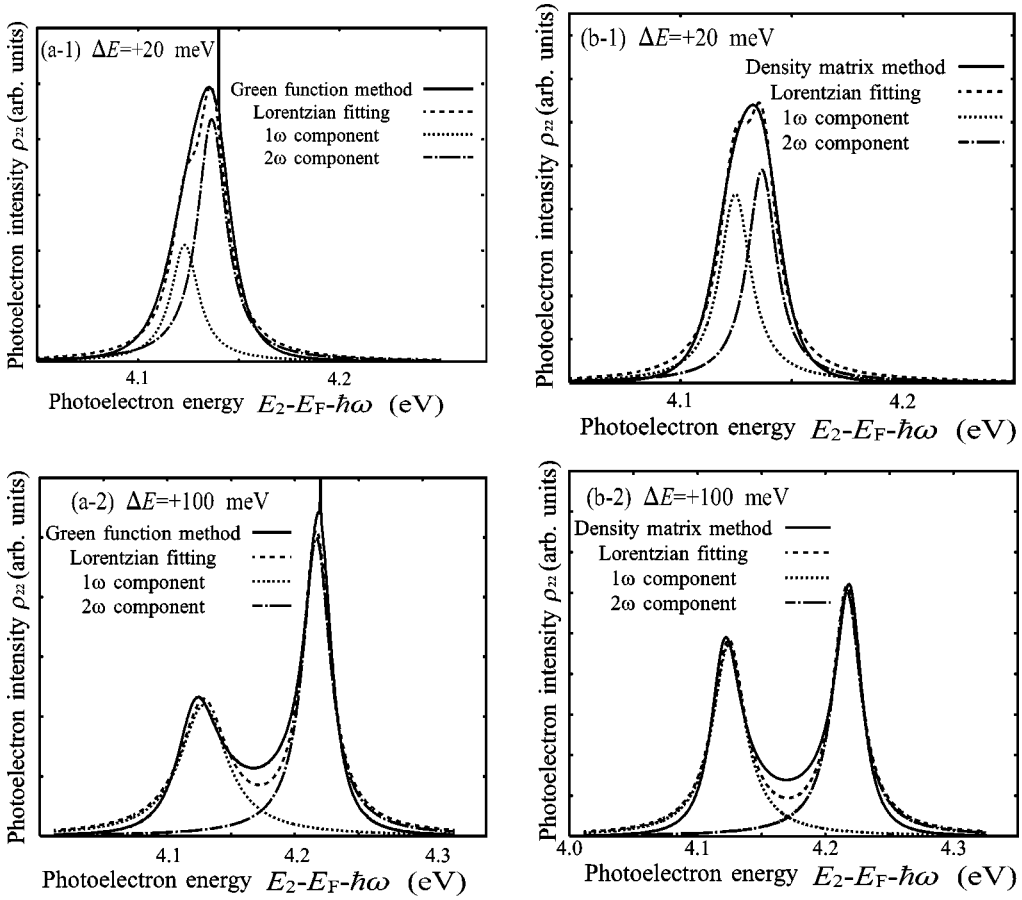

FIG. 2. Lorentzian fitting to the 2PPE spectra for $\Delta E=+20$ and $+100$ meV obtained by (a) the Green function method and (b) the density matrix method. The decomposed peak components are also shown.

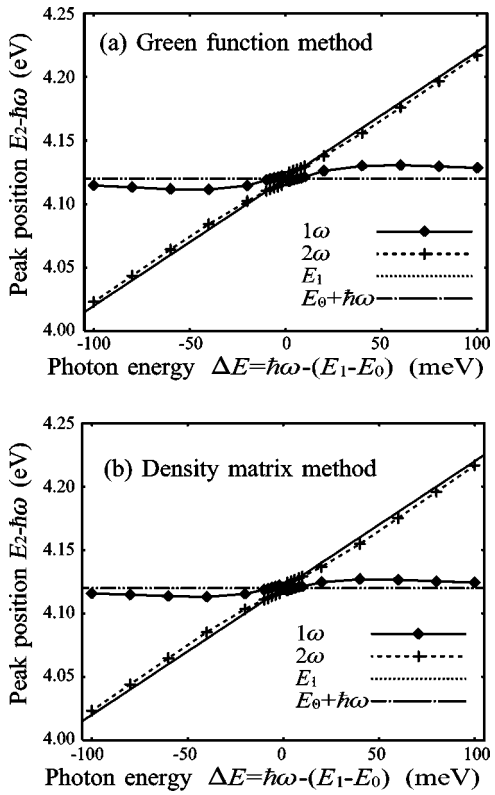

FIG. 3. Energy positions of the 1ω and 2ω peaks as functions of $\hbar\omega$ decomposed from the results by (a) the Green function method and (b) the density matrix method. The peak positions in the absence of the interference effects, i.e., $E_2=E_1+\hbar\omega$ for the 1ω peak and $E_2=E_0+2\hbar\omega$ for the 2ω peak, are also shown.

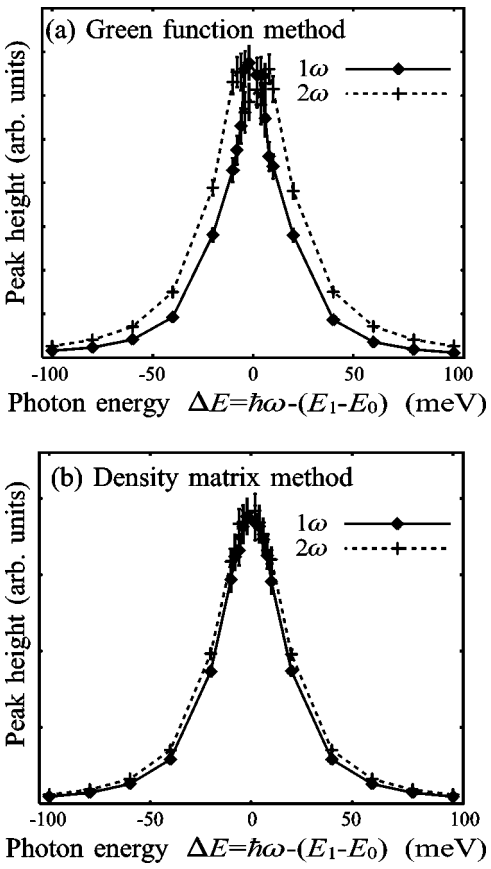

FIG. 4. Heights of the 1ω and 2ω peaks as functions of $\hbar\omega$ decomposed from the results by (a) the Green function method and (b) the density matrix method. The error bars for the Lorentzian fitting are also shown.

exhibit two peaks both in the results by the Green function method and the density matrix method [see Figs. 2(a-2) and 2(b-2)]. The symptom of the sharpening of the spectra at the resonance is manifested in the middle of the energy region between the peaks ($\sim$4.17 eV). This accounts for the attraction between the two peaks. The qualitative features of the spectra are similar between the Green function method and the density matrix method; however, we see a difference in the 1ω peak width. As discussed later, this difference is concerned with the details of the process accounting for the 1ω peak. In this paper, we do not discuss the difference of the ratio between the 1ω and 2ω peak heights which can largely depend on the approximation employed in the calculation of Eq. (12).

Here we investigate the photon energy dependence of the peak positions of the 1ω and 2ω peaks (see Fig. 3). In the absence of the interference effects, the 1ω and 2ω peaks will be located at $E_1+\hbar\omega$ and $E_0+2\hbar\omega$, respectively. The obtained peak positions shift from these values by the attraction between the peaks due to the interference as seen from Fig. 2. When the detuning is smaller than the linewidths of the occupied and unoccupied states, both the 1ω and 2ω components shift with the gradient of 1.5 because of the coupling between the two components.

The resonance curves (peak heights as functions of $\hbar\omega$) for the two peaks are shown in Fig. 4. Both the 1ω and 2ω resonance curves mainly reflect the transition probability of the excitation from $|0\rangle$ to $|1\rangle$ by the first photon, $\propto[(E_1-E_0-\hbar\omega)^2+(\Gamma_1+\Gamma_0)^2]^{-1}$. When we ignore the region of $|\Delta E|<10$ meV where the fitting errors are large, the resonance curves for the both two peaks can be fitted by a Lorentzian of which the full widths at half maximum is 40 meV. The narrowing of the curves from $2(\Gamma_1+\Gamma_0)=54.0$ meV is due to the interference effect that accounts for the enhancement of the photoelectron intensity around the resonance.

The dependence of the full widths at half maximum of the 1ω and 2ω peaks on the photon energy is shown in Fig. 5. The widths in the vicinity of the resonance photon energy, $\sim$15 meV, are smaller than the electron linewidth $2\Gamma_1=28.6$ meV and hole linewidth $2\Gamma_0=25.3$ meV. This is due to the interference effect that accounts for the narrowing of the peak structure.

For the large detuning, the 2ω peak width converges into a value (25.5 meV at $|\Delta E|=400$ meV). This value corresponds to $2\Gamma_0$ in the Green function method and $2\bar{\gamma}$ in the density matrix method. Thus we see a relation, $\bar{\gamma}=\Gamma_0$. While the 1ω peak width in the density matrix method converges into $2\Gamma_1$, the 1ω peak width in the Green function method show an asymmetric behavior with respect to the resonance photon energy. This reflects the detail of the scattering processes accounting for the dephasing. Approximately, the 1ω

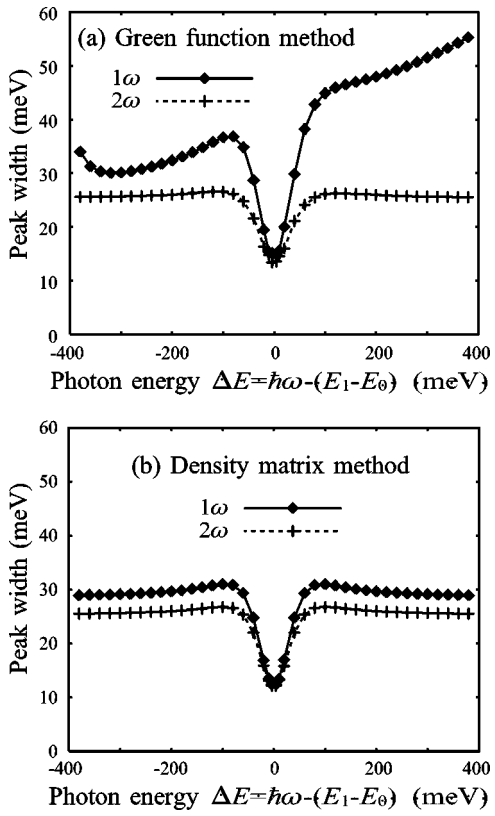

FIG. 5. Full widths at half maximum of the 1ω and 2ω peaks as functions of $\hbar\omega$ decomposed from the results by (a) the Green function method and (b) the density matrix method. The increase of the 1ω peak width at $\Delta E \sim -400$ meV in the Green function method is due to the misfit to the broken peak structure near the Fermi cutoff.

peak width for $|\Delta E| > 100$ meV is given by $2\Gamma_1 + 2\bar{\Gamma}_0(\Delta E)$, where $\bar{\Gamma}_0(\Delta E) = \alpha|\Delta E + (E_F - E_0)|^2$ corresponds to the available phase space of the hole scattering at $|0\rangle$ given with a proportional coefficient α (confirmed from a graph in a range wider than Fig. 5).

In the usual analysis of the (time-resolved) 2PPE spectra, the relaxation time is assumed to be the electron lifetime, i.e., $\gamma_1 = \Gamma_1$. This assumption is correct at the lowest limit of the photon energy for which the 1ω peak structure is not collapsed by the Fermi cutoff. When the detuning is large, the 1ω peak collapses due to the large scattering probability and hence the width becomes large and the intensity becomes weak (13% of the 2ω peak at $\Delta E = +400$ meV).

The inelastic scattering of the hole does not affect the intrinsic lifetime of the electron in $|1\rangle$, however, the hole scattering can affect the electron densities and the polarizations by changing the quantum phase of the system. In the time-resolved 2PPE spectra, the hole scattering accounts for a narrowing of the pump-probe correlation traces similar to the narrowing due to the pure dephasing in the density matrix method.[12] The results in previous studies and in the present study, confirm the expectation that the inelastic hole scattering can account for dephasing.

Usually, the physical mechanism of the occurrence of the 1ω peak is explained by the step-by-step processes[8] associated with cascade and Auger processes that electron transfer to $|1\rangle$ occurs by scattering of electrons or holes photoexcited outside of the partial system consisting of $|1\rangle$ and $|0\rangle$.[7] These processes will compete with the hole scattering processes considered in the present work, and can be represented by extended formulas of ρ_{22} including vertices striding over the forward and backward branches of the Keldysh contour.[18] The height of the 1ω peak due to the cascade and Auger processes will be less dependent on $\hbar\omega$ around $E_1 - E_0$ than the peak due to the hole scattering processes in the present work. Therefore, these processes may be distinguished by measuring the $\hbar\omega$ dependence of the peak heights and widths,[1,3,4] however, it will be an issue in the future to accumulate sufficient amount of high-resolution experimental spectra to compare with the theories.

IV. CONCLUSIONS

By investigating the 2PPE energy spectra of Cu(111), we showed that inelastic scattering of a photoexcited hole in an occupied state at metal surfaces accounts for dephasing. The density matrix method qualitatively reproduces the results by the nonequilibrium Green function method when we assume that the energy relaxation time is equal to the electron lifetime in the unoccupied state and the dephasing time is equal to the hole lifetime in the occupied state. Then we can confirm that the 2ω peak width corresponds to the hole linewidth when the detuning is large.

The 1ω peak width, which corresponds to the energy relaxation time γ_1 in the density matrix method, shows a remarkable dependence on the photon energy in the Green function method. In a previous study on the time-resolved 2PPE spectra for femtosecond laser pulses, we showed that the energy relaxation time γ_1 corresponds to a lifetime of the polarization consisting of the electron and the hole, i.e., $\gamma_1 = \Gamma_1 + \Gamma_0$. On the other hand, in the present study on the energy-resolved spectra for continuous light, we showed $\gamma_1 = \Gamma_1 + \bar{\Gamma}_0(\Delta E)$, where the available phase space $2\bar{\Gamma}_0(\Delta E)$ for the hole scattering as a function of the detuning ΔE is not exactly the intrinsic hole linewidth $2\Gamma_0$ itself. The reasons for the difference between these results will be related with the limitation of the macroscopic model and the mathematical problem in treatment of the dephasing terms in the density matrix method as explained in the Appendix.

ACKNOWLEDGMENTS

One of the authors (M.S.) acknowledges the support by the Special Postdoctoral Researchers Program of RIKEN. This work was partly supported by the Ministry of Education, Culture, Sports, Science and Technology of Japan, through their Grant-in-Aid for COE Research (10CE2004), Scientific Research (11640375) programs, and by the New Energy and Industrial Technology Development Organization (NEDO), through their Materials and Nanotechnology program, and by the Japan Science and Technology Corporation (JST), through their Research and Development Applying Advanced Computational Science and Technology program.

APPENDIX: MACROSCOPIC THEORY BY THE DENSITY MATRIX METHOD

In this appendix, we derive the formula of the 2PPE spectra by the density matrix method which is usually used for an analysis of the experimental data. We introduce the unperturbed Hamiltonian H_0 in Eq. (1) and the interactions of an electron with light W in Eq. (3) in the same way as in Sec. II, whereas we introduce phenomenological inverse relaxation times and dephasing times instead of the Coulomb interactions between electrons V in Eq. (2).

The Liouville–von Neumann equations in the Schrödinger representation for describing the 2PPE from an open two-level system consisting of an occupied state $|0\rangle$ and an unoccupied state $|1\rangle$ at the surface are given by

$$i\hbar \frac{\partial \rho_{\mu\nu}(t)}{\partial t} = [H_0 + W(t), \rho(t)]_{\mu\nu} - i\gamma_{\mu\nu}\rho_{\mu\nu}(t) \quad (\mu,\nu = 0,1,2 \quad \text{except for} \quad \mu=\nu=0), \tag{A1}$$

and $\rho_{00}(t) \simeq 1$. Here the diagonal elements of γ give the inverse energy relaxation times by $\gamma_{22} = 2\gamma_2$ and $\gamma_{11} = 2\gamma_1$. The off-diagonal elements give the inverse dephasing times by $\gamma_{12} = \gamma_{21} = \gamma_1$, $\gamma_{01} = \gamma_{10} = \gamma_1 + \overline{\gamma}$, and $\gamma_{02} = \gamma_{20} = \gamma_2 + \overline{\gamma}$, where $\overline{\gamma}$ is an inverse pure dephasing time between $|1\rangle$ and $|0\rangle$. In the following, from the point of view of the Green function method, we derive the formulas of the photoelectron density corresponding to those obtained by Ueba *et al.*[8] For simplicity, we ignore the pure dephasing between $|2\rangle$ and $|1\rangle$,[2,5,6] so that we can obtain formulas of the photoelectron density comparable with those obtained by the Green function method.

We obtain the photoelectron density within the fourth order with respect to W by calculating $\rho_{01} = \rho_{10}^*$, ρ_{11}, $\rho_{02} = \rho_{20}^*$, $\rho_{12} = \rho_{21}^*$, and ρ_{22} in order. Then we derive a formula of the photoelectron density equivalent to Eq. (5) where Γ_1 is replaced with γ_1 and $G_{00}^{+-}(t_{ob}-t, t'-t_{ob})$ is replaced with

$$\overline{G}_{00}^{+-}(t-t') = -(i\hbar)^{-1}\theta(E_F - E_0)e^{-iE_0(t-t')/\hbar - \overline{\gamma}|t-t'|/\hbar}. \tag{A2}$$

Then the Fourier transform of this Green function becomes a function of one energy in the same way as in Eq. (10) whereas G_{00}^{+-} was a function of two energies.

By substituting the inverse transform of Eq. (10) for $G^{++}(\tau)$, $G^{--}(\tau)$, and $\overline{G}^{+-}(\tau)$, Eq. (5) is rewritten as

$$\rho_{22}[E_2] = \mathrm{Re}\left[\frac{i}{(2\pi)^5} |W_{21}W_{10}|^2 \int_{C_+} d\epsilon_2 \int_{C_+} d\epsilon_1 \int_{C_+} d\epsilon_0 \times \int_{C_-} d\epsilon_1' \int_{C_-} d\epsilon_2' G_{22}^{++}[\epsilon_2] G_{11}^{++}[\epsilon_1] \overline{G}_{00}^{+-}[\epsilon_0] \times G_{11}^{--}[\epsilon_1'] G_{22}^{--}[\epsilon_2'] \frac{1}{\epsilon_1 - \epsilon_1' + i0_+} \frac{1}{\epsilon_2 - \epsilon_2' + i0_+} \times \frac{1}{\epsilon_1' + \hbar\omega - \epsilon_0 - i0_+} \left[\frac{1}{\epsilon_2 + \hbar\omega - \epsilon_1' + i0_+} + \frac{(\epsilon_1 - \epsilon_1' + i0_+) - (\epsilon_2' + 2\hbar\omega - \epsilon_0 - i0_+)}{(\epsilon_2' + \hbar\omega - \epsilon_1 - i0_+)(\epsilon_2' + 2\hbar\omega - \epsilon_0 - i0_+)} \right] \right]. \tag{A3}$$

The complexity of this equation is due to the $|t-t'|$ dependence of $\overline{G}^{+-}$. By using Eqs. (6) and (A2), we obtain

$$\rho_{22}[E_2] = \frac{|W_{21}W_{10}|^2}{(E_2 - E_1 - \hbar\omega)^2 + (\gamma_2 + \gamma_1)^2} \left\{ \frac{\gamma_1 + \overline{\gamma}}{\gamma_1} \frac{1}{(E_1 - E_0 - \hbar\omega)^2 + (\gamma_1 + \overline{\gamma})^2} + \frac{\gamma_2 + \overline{\gamma}}{\gamma_2} \frac{1}{(E_2 - E_0 - 2\hbar\omega)^2 + (\gamma_2 + \overline{\gamma})^2} + \frac{(\gamma_1 + \overline{\gamma})(\gamma_2 + \overline{\gamma}) - (E_1 - E_0 - \hbar\omega)(E_2 - E_0 - 2\hbar\omega)}{[(E_1 - E_0 - \hbar\omega)^2 + (\gamma_1 + \overline{\gamma})^2][(E_2 - E_0 - 2\hbar\omega)^2 + (\gamma_2 + \overline{\gamma})^2]} \right\}. \tag{A4}$$

Usually, γ_2 is given to be infinitesimal since it is considered that the photoelectrons emitted into the vacuum cannot be scattered by other electrons in the metal. In this case, the second term in the brace of Eq. (A4) becomes dominant:

$$\rho_{22}[E_2] \propto \frac{1}{(E_2 - E_1 - \hbar\omega)^2 + \gamma_1^2} \frac{1}{(E_2 - E_0 - 2\hbar\omega)^2 + \overline{\gamma^2}}. \tag{A5}$$

This reproduces the qualitative feature of the experimental 2PPE spectra exhibiting both 1ω and 2ω peaks in the same way as the results by the Green function method. However, the absolute value of ρ_{22} becomes infinite for any E_2 due to the coefficient $(\gamma_2 + \overline{\gamma})/\gamma_2$ whereas this problem has not arisen in the case of the laser pulses with finite duration. On the other hand, when $\overline{\gamma} \to 0$ (before $\gamma_2 \to 0$), Eq. (A4) is rewritten as

$$\rho_{22}[E_2]=|W_{21}W_{10}|^2\frac{1}{(E_1-E_0-\hbar\omega)^2+\gamma_1^2}\times\frac{1}{(E_2-E_0-2\hbar\omega)^2+\gamma_2^2}, \quad \text{(A6)}$$

which exhibits only the 2ω peak and the absolute value of ρ_{22} is finite at $E_2\neq E_0+2\hbar\omega$ even when $\gamma_2\to 0$.

This unnatural property of ρ_{22} is concerned with the formula of $\bar{G}_{00}^{+-}$ in Eq. (A2) leading to the unsuccessful expression Eq. (A3) in the Fourier domain (this problem would have been overlooked in many theories on nonequilibrium systems) but not due to the neglect of dephasing between $|2\rangle$ and $|1\rangle$ nor due to the neglect of higher order terms with respect to W and γ. By comparing Eq. (A3) with Eq. (11), we see that the time evolutions in the bra and ket vectors are not distinguished properly in the density matrix method. This means that the effects of the interference between scattering processes accounting for the dephasing are not estimated properly by the density matrix method. Thus the unnatural properties are due to the mathematical forms of the dephasing terms which are usually introduced in the Liouville-von Neumann equations.

As well as the density matrix methods, in the usual nonequilibrium Green function methods where the dependence of the Green functions on the observation time is not considered,[18,19] and hence the formula of G_{00}^{+-} is assumed to be equivalent to Eq. (A2), one will obtain results similar to Eq. (A4). Thus, even though the experimental data seem to be reproduced fortunately,[10] regarding the effects of dephasing it will be necessary to reconsider the results of 2PPE spectra obtained so far by the usual methods.

*Present address: Japan Science and Technology Agency, Kawaguchi, Saitama 332-0012, Japan. Electronic address: sakaue@aria.mp.es.osaka-u.ac.jp

[1] W. Steinmann, Appl. Phys. A: Solids Surf. **49**, 365 (1989).
[2] M. Wolf, E.K.A. Hotzel, and D. Velic, Phys. Rev. B **59**, 5926 (1999).
[3] T. Munakata, Surf. Sci. **454–456**, 118 (2000).
[4] W. Wallauer and T. Fauster, Surf. Sci. **374**, 44 (1997).
[5] H. Ueba, Surf. Sci. **334**, L719 (1995).
[6] K. Boger, M. Roth, M. Weinelt, and T. Fauster, Phys. Rev. B **65**, 075104 (2002).
[7] M. Sakaue, H. Kasai, and A. Okiji, Appl. Surf. Sci. **169–170**, 68 (2001).
[8] H. Ueba and T. Mii, Appl. Phys. A: Mater. Sci. Process. **71**, 537 (2000).
[9] A. M. Zagoskin, *Quantum Theory of Many-Body Systems* (Springer-Verlag, New York, 1998).
[10] M. Sakaue, T. Munakata, H. Kasai, and A. Okiji, Phys. Rev. B **66**, 094302 (2002).
[11] M. Sakaue, T. Munakata, H. Kasai, and A. Okiji, Surf. Sci. **507–510**, 740 (2002).
[12] M. Sakaue, T. Munakata, H. Kasai, and A. Okiji, Surf. Sci. **532–535**, 30 (2003).
[13] M. Sakaue, H. Kasai, and A. Okiji, J. Phys. Soc. Jpn. **68**, 720 (1999).
[14] P.M. Echenique, J. Osma, M. Machado, V.M. Silkin, E.V. Chulkov, and J.M. Pitarke, Prog. Surf. Sci. **67**, 271 (2001).
[15] E.V. Chulkov, V.M. Silkin, and M. Machado, Surf. Sci. **482–485**, 693 (2001).
[16] H. Petek and S. Ogawa, Prog. Surf. Sci. **56**, 239 (1997).
[17] A. A. Abrikosov, L. P. Gor'kov, and I. Y. Dzyaloshinskii, *Quantum Field Theoretical Methods in Statistical Physics* (Pergamon, New York, 1965).
[18] M. Sakaue, H. Kasai, and A. Okiji, J. Phys. Soc. Jpn. **69**, 160 (2000).
[19] Y.J. Dappe, A.A. Villaeys, and F.P. Lohner, Appl. Surf. Sci. **168**, 41 (2000).